Chemical Science

ROYAL SOCIETY OF CHEMISTRY

EDGE ARTICLE

View Article Online
View Journal | View Issue

Cite this: *Chem. Sci.*, 2021, **12**, 10266

All publication charges for this article have been paid for by the Royal Society of Chemistry

Received 8th April 2021
Accepted 24th June 2021

DOI: 10.1039/d1sc01974k

rsc.li/chemical-science

Photocatalytic deoxygenation of N–O bonds with rhenium complexes: from the reduction of nitrous oxide to pyridine *N*-oxides†

Marianne Kjellberg, Alexia Ohleier, Pierre Thuéry, Emmanuel Nicolas, Lucile Anthore-Dalion * and Thibault Cantat *

The accumulation of nitrogen oxides in the environment calls for new pathways to interconvert the various oxidation states of nitrogen, and especially their reduction. However, the large spectrum of reduction potentials covered by nitrogen oxides makes it difficult to find general systems capable of efficiently reducing various *N*-oxides. Here, photocatalysis unlocks high energy species able both to circumvent the inherent low reactivity of the greenhouse gas and oxidant N_2O ($E^0(N_2O/N_2) = +1.77$ V *vs.* SHE), and to reduce pyridine *N*-oxides ($E_{1/2}$(pyridine *N*-oxide/pyridine) = −1.04 V *vs.* SHE). The rhenium complex [Re(4,4′-*t*Bu-bpy)$(CO)_3$Cl] proved to be efficient in performing both reactions under ambient conditions, enabling the deoxygenation of N_2O as well as synthetically relevant and functionalized pyridine *N*-oxides.

Introduction

The modern development of intensive soil exploitation and – in corollary – the massive production of nitrogen-based fertilizers from atmospheric N_2 has enabled us to feed an ever-growing population.[1] Collateral damage, however, includes increased production and accumulation of noxious nitrogen oxide wastes such as nitrates NO_3^-, nitrites NO_2^- or nitrous oxide N_2O, their reduction back to N_2 being mostly ensured by the natural nitrogen cycle.[2] As defined by environmental scientists, planetary boundaries for the biogeochemical nitrogen cycle have indeed already been crossed, the current nitrogen anthropogenic fixation representing more than twice the estimated boundary (150 Tg N per year *vs.* 62 Tg N per year).[3] Since breaking the highly stable N_2 bond *via* the Haber–Bosch process consumes yearly 2% of worldwide energy, leakage of nitrogen oxides in the environment also represents a loss of energy.[4] In the search for a more sustainable economy, there is hence a need for new pathways able to perform efficient interconversion between oxidation states of nitrogen, and especially reduction of nitrogen oxides to less oxidized molecules.[5]

Chemically speaking, this raises the issue of deoxygenating the N–O bond of both inorganic and organic *N*-oxides. With the aim to explore new pathways, we decided to harness the potential of homogeneous photoredox catalysis. One of its most important applications is the deoxygenation of C–O bonds of C_1-molecules, which covers a narrow spectrum of reduction potentials (0.4 V, Fig. 1a).[6] The main strategy in optimizing photo- or electro-catalysts has thus been focused on the selectivity between different products, especially between CO and HCOOH.[7] Nitrogen oxides however cover a wider spectrum of reduction potentials (over 2.8 V, Fig. 1a) shifting the question from a search for selective catalysts, to the discovery of versatile catalytic systems.[8]

A simple model that can be used to showcase this deoxygenation is the ozone-depleting nitrous oxide N_2O, since it leads directly to N_2. Although N_2O is a strong oxidant ($E^0(N_2O/N_2) = +1.77$ V *vs.* SHE),[8] homogeneous deoxygenation reactions are scarcely reported, for it is highly inert and a poorly coordinating molecule.[9] Among the few thermocatalytic deoxygenating methods, Milstein group disclosed the hydrogenation of N_2O to N_2 and H_2O catalyzed by a PNP pincer ruthenium complex at 65 °C, under a total pressure of 7 bar (Fig. 1b).[10] More recently, our laboratory proposed the deoxygenation of N_2O using disilanes and a catalytic amount of fluoride source under ambient conditions (Fig. 1b).[11] To the best of our knowledge, only heterogeneous photodeoxygenation of N_2O has been so far reported.[12] A very recent report by the group of Costentin and Chardon-Noblat demonstrated the use of Re^I complexes able to catalyse the electroreduction of N_2O to N_2.[13]

At the opposite end of the redox scale, pyridine *N*-oxides have, in contrast, considerably lower reduction potentials ($E_{1/2}$(pyridine *N*-oxide (**1a**)/pyridine (**2a**)) = −1.04 V *vs.* SHE, Fig. 1b) and they represent a much greater challenge.[14] These compounds are useful intermediates in the synthesis of N-heteroaromatic-containing pharmaceutical or agrochemical products, where *N*-oxides are used for instance as directing

Université Paris-Saclay, CEA, CNRS, NIMBE, 91191 Gif-sur-Yvette CEDEX, France

† Electronic supplementary information (ESI) available: Data relating to the characterization data of materials and products, general methods, optimization studies, experimental procedures, gas chromatography, NMR spectra, and CIF X-ray structures. CCDC 2056048 and 2056049. For ESI and crystallographic data in CIF or other electronic format see DOI: 10.1039/d1sc01974k

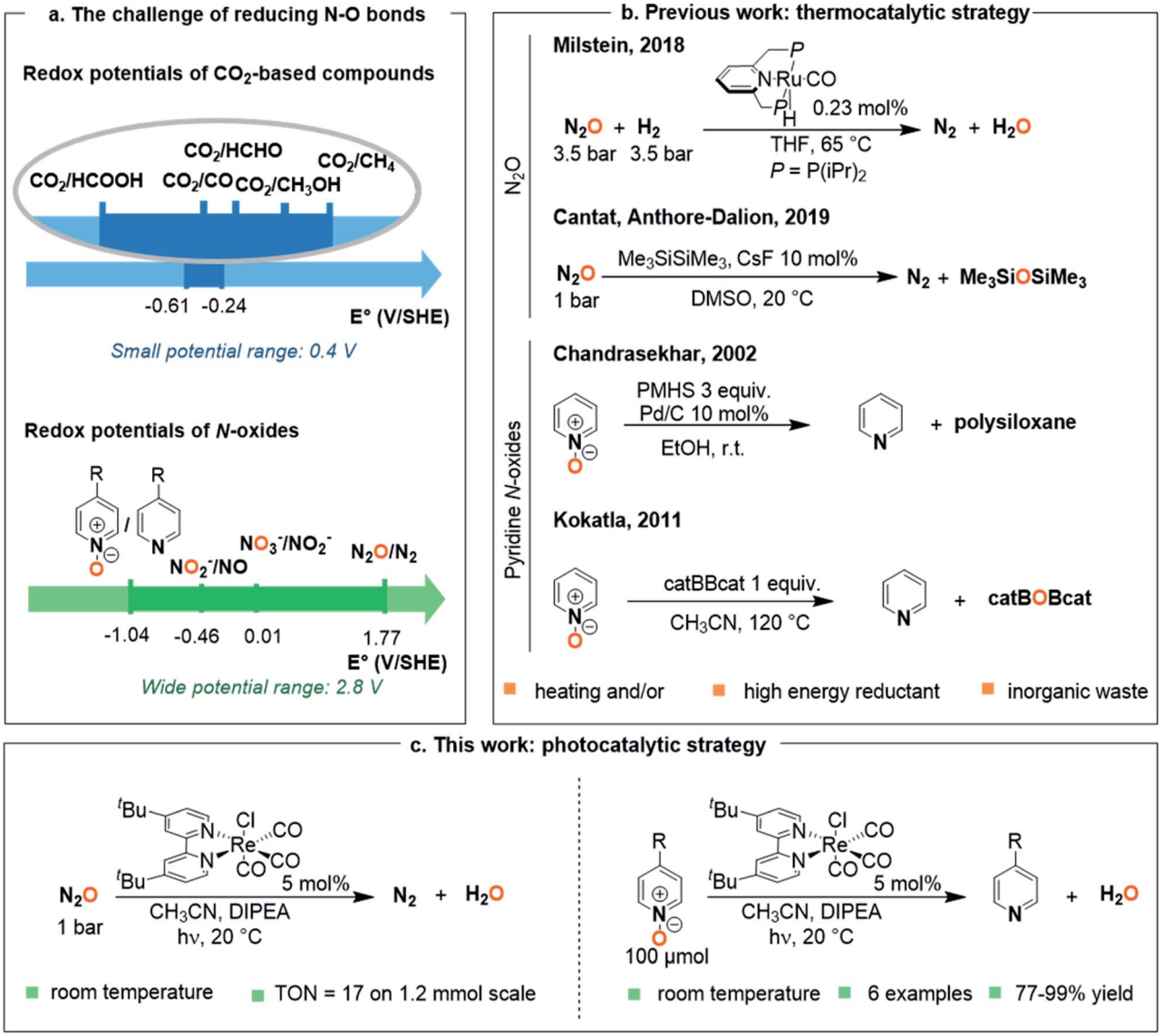

Fig. 1 Development of a photocatalytic pathway to deoxygenate N–O bonds. (a) Range of potentials involved for the reduction of C–O and N–O bonds. (b) Existing strategies for N–O bond deoxygenation. (c) Proposed strategy for the deoxygenation of N_2O and pyridine *N*-oxides. DIPEA, diisopropylethylamine.

groups for C–H bond functionalization.[15] In that context, there is a need for mild methods to post-reduce the *N*-oxide group and afford the N-heterocycle. The main reported methods involve sacrificial oxophilic reagents or high energy reductant based on phosphines,[16] silane[17] or borane[18] derivatives, with thermochemical or (photo)electrochemical activation.[19] Nevertheless, all these methods imply the use of either heating systems or high energy reductants (with $E^0 < 0$ V), leading to a loss of energy. There is moreover no report of systems capable of addressing the wide range of potentials (>2.5 V) required to reduce both nitrous oxide and pyridine *N*-oxides.

Herein, we demonstrate that a versatile photocatalytic system based on [Re(bpy)(CO)$_3$Cl]-type complexes[20] is able to efficiently deoxygenate both N_2O and pyridine *N*-oxides under ambient conditions (20 °C, 1 bar, Fig. 1c).

Results and discussion

Design of the system for the photodeoxygenation of N_2O

The potential of [Re(bpy)(CO)$_3$Cl] (**Re-1**) to photocatalyze the conversion of N_2O to N_2 was tested, using **Re-1** (5 mol%) as catalyst in acetonitrile in the presence of triethanolamine (TEOA) and 1 bar of N_2O. After 2 h of irradiation with white LEDs at 20 °C, N_2 was formed to our delight in 66% yield according to GC analysis of the gaseous fraction. This result represents the first homogeneous photocatalytic deoxygenation of N_2O to N_2 (Table 1, entry 1).

In the absence of **Re-1**, no conversion of N_2O was observed: cleavage of the N–O bond does not occur spontaneously under irradiation (Table 1, entry 2). Other blank experiments

Table 1 Photodeoxygenation of N_2O catalyzed by Re-1 and control experiments

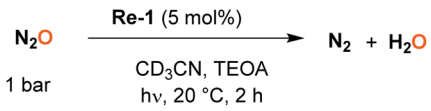

Entry	Deviation from standard conditions[a]	% H_2[b]	% N_2[b]	% N_2O[b]
1	None	1.5	66	32
2	No photocatalyst	0	2	98
3	No light	0	4	96
4	No N_2O[c]	91	9	0
5	No TEOA	0	8	92
6	TEA instead of TEOA	0.2	36	63
7	**DIPEA instead of TEOA**	**0**	**76**	**24**

[a] Standard reaction conditions: N_2O (1 bar, 100 μmol), **Re-1** (5 μmol, 5 mol%), donor (570 μmol, 5.7 equiv.), CD_3CN (0.5 mL), 2 h, 20 °C. [b] Determined by GC analysis of the gaseous phase. Percentages correspond to the fraction of named gas in the overall analyzed gaseous phase (corrected with response factors). [c] Under argon (1 bar). TEOA: triethanolamine; TEA: trimethylamine; DIPEA: diisopropylethylamine.

confirmed that no N_2 is formed in the absence of light, N_2O, or electron donor (Table 1, entries 3–5).

Interestingly, the reaction performed without N_2O afforded H_2 as sole product, as a result of TEOA decomposition in the presence of the catalyst under irradiation (Table 1, entry 4). The detection of traces of H_2 at the end of the reaction (1.5% of the gaseous phase, Table 1, entry 1) was thus ascribed to the use of TEOA. Sacrificial amines in photocatalysis are indeed known to supply the catalytic cycle with electrons and may serve as a proton source, which can in turn be reduced by the photocatalyst to H_2.[6a,21] This prompted us to investigate the influence of the sacrificial electron donor on the outcome of N_2O photocatalytic reduction. Another tertiary amine, triethylamine (TEA), was used, inducing a drop of the N_2O conversion, the gaseous fraction of N_2 after 2 h decreasing from 66% to 36% without suppressing the generation of H_2 (Table 1, entry 6). Interestingly, when a bulkier tertiary amine, diisopropylethylamine (DIPEA, Hünig's base), was used as electron donor, H_2 could not be detected in GC after 2 hours of irradiation, and the N_2 yield increased up to 76% (Table 1, entry 7). We therefore selected DIPEA as the sacrificial electron donor for the rest of our study.

Catalyst optimization

When the reaction was scaled up from 0.1 to 1.2 mmol N_2O, the yield with **Re-1** as catalyst dropped to 50%, affording a TON of 10 and a TOF_0 of 1.9 h^{-1} (Table 2, entry 1). GC-monitoring showed no evolution after 22 h of reaction, indicating potential deactivation of the catalyst. We hence explored the effects of substitution on the bipyridine ligand. We synthesized a series of [Re(bpy)$(CO)_3$Cl]-type catalysts with bipyridines substituted either on the 4,4′ or the 6,6′-position, and we studied their ability to photocatalyze the deoxygenation of N_2O (Fig. 2a).

Table 2 Performances of the photocatalysts in the deoxygenation of N_2O[a]

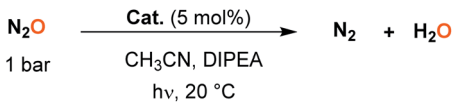

Entry	Catalyst	TOF_0 (h^{-1})	% N_2 (TON)	Time (h)
1	**Re-1**	1.9	50 (10)	22
2	**Re-2**	3.7	70 (14)	50
3	**Re-3**	**4.3**	**86 (17)**	**115**
4	**Re-4**	2.7	55 (11)	100
5	**Re-5**	1.1	61 (12)	150

[a] Reaction conditions: N_2O (1.0 bar, 1.2 mmol), catalyst (60 μmol, 5 mol%), DIPEA (6.9. mmol, 5.7 equiv.), CH_3CN (6 mL), 20 °C.

Complexes **Re-2** (ref. 22) and **Re-3**,[23] possessing bipyridines substituted in the 4,4′-position with methyl or *t*-butyl groups, respectively, were also active in the deoxygenation of N_2O, and led to higher yields in N_2 than unsubstituted **Re-1**, 70% and 86% respectively, corresponding to TONs of 14 and 17. They also showed higher activity than **Re-1**: TOF_0 reached 3.7 h^{-1} and 4.3 h^{-1} for **Re-2** and **Re-3** respectively *vs.* 0.7 h^{-1} for **Re-1** (Table 2, entries 1–3). On the other hand, **Re-4** (ref. 23) and the novel **Re-5** complex, featuring methyl and bulky mesityl substituents in the 6 and 6′ positions of bipyridines, were less efficient on a 24 h timescale, leading to moderate yields in N_2 of 55% and 61% respectively (Table 2, entries 4 and 5). This behavior is also present in their initial activities: lower TOF_0 (2.7 and 1.1 h^{-1} for **Re-4** and **Re-5** respectively) were measured compared to **Re-2** and **Re-3**.

A more precise monitoring of kinetic profiles for each catalyst was also performed (Fig. 2b). The evolution of the N_2 yield over 60 h showed that **Re-1** deactivated after 22 h, sooner than all the other substituted catalysts, which accounts for the low yields obtained with **Re-1**. In contrast, **Re-2** and **Re-3**, presenting *para*-substituted bipyridines, showed both high catalytic activity and increased stability. A possible explanation of this phenomenon has been studied in the case of CO_2 electroreduction by Kubiak *et al.*: they showed that substituting the bipyridine ligand in the 4,4′-positions provided sufficient steric hindrance to inhibit the dimerization of a Re(0) reactive intermediate to an inactive bimetallic complex.[24,25] The stability increased with the steric bulk of the substituent. The same tendency is observed here in the case of the photoreduction of N_2O, and hints towards a similar mechanistic pathway. Complexes **Re-4** and **Re-5**, substituted in the *ortho* position, demonstrated an increased stability compared to **Re-1** but, interestingly enough, the increase in stability brought by substitution on the bipyridine did not come along with an increase in activity. These catalysts indeed required respectively 100 h and 150 h to yield 55% and 61% of N_2. A structural explanation could arise from the steric strain between the substituents on the bipyridine and the equatorial carbonyls in **Re-4** and **Re-5**.[26]

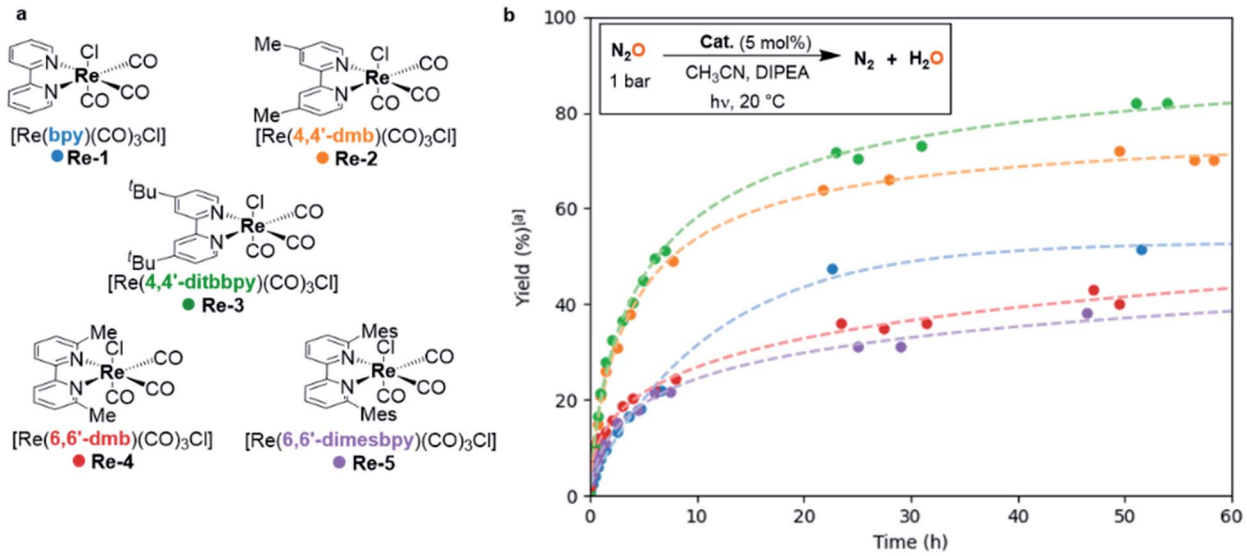

Fig. 2 Photodeoxygenation of N_2O: screening of catalysts. (a) Photocatalysts **Re-1–5** used in the study. (b) Kinetic profiles on 1.2 mmol scale. Reaction conditions: N_2O (1.0 bar, 1.2 mmol), catalyst (60 μmol, 5 mol%), DIPEA (6.9 mmol, 5.7 equiv.), CH_3CN (6 mL), 20 °C.

Rhenium photocatalysts of type $[Re(bpy)(CO)_3Cl]$ are thus able to catalyze the deoxygenation of N_2O, suggesting that other N–O bonds could be deoxygenated under similar reaction conditions.

Photodeoxygenation of pyridine *N*-oxides

Encouraged by the success of N_2O deoxygenation, and to probe the versatility of our catalytic system, we considered the possibility of applying this methodology to the deoxygenation of more challenging N–O bonds across the scale of redox potentials, namely of pyridine *N*-oxides ($E_{1/2}$(pyridine *N*-oxide (**1a**)/pyridine (**2a**)) = −1.04 V *vs.* SHE).

The reaction was monitored by NMR using rhenium-based **Re-1–5** photocatalysts. To our delight, a first attempt using the *t*Bu-substituted catalyst **Re-3** under the reaction conditions developed for N_2O enabled deoxygenation of pyridine *N*-oxide (**1a**) to pyridine (**2a**) in 82% yield after 34 h (Table 3, entry 1). The blank experiments confirmed that all components (light, photocatalyst, electron donor) were necessary to perform the reduction (see ESI Table S1†). Remarkably, the other catalysts also afforded full conversion of compound **1a**, albeit with longer reaction times (44–87 h), leading to pyridine (**2a**) in 85–99% yield (Table 3, entries 2–5). This stands in contrast with our observations with N_2O: here the yields showed steady increase until full conversion with all catalysts. Two explanations may account for this phenomenon: either the pyridine produced during the reaction delays catalyst deactivation through the stabilization of reactive intermediates,[27] or the higher oxidative character of N_2O has a detrimental effect on the catalyst stability. This effect was particularly beneficial in the case of the 6,6′-dimethylbipyridine rhenium complex **Re-4**, which led only to 55% yield of N_2 after 100 h and gave full conversion of pyridine *N*-oxide (**1a**) within 55 h. Again, 4,4′-substituted catalysts **Re-2** and **Re-3** displayed higher catalytic activity (TOF_0 = 11 and 16 h^{-1}) than unsubstituted **Re-1** and 6,6′-substituted **Re-4** and **Re-5** (TOF_0 = 5.5, 7.5 and 2.6 h^{-1}, respectively), suggesting similar mechanistic patterns for the deoxygenation of both N_2O and pyridine *N*-oxide (**1a**) (Table 3). To study the effect of irradiation, a light on/light off experiment was also performed (Fig. 3a).[28] The substrate was only converted when the system was exposed to light, and the reaction stopped once the system was in the dark. Continuous irradiation is thus required to perform the reaction.

Table 3 Photocatalytic deoxygenation of pyridine *N*-oxide with different photocatalysts[a]

Entry	Cat.	TOF_0 (h^{-1})	Yield (%)	Time to full conversion (h)
1	**Re-3**	16	82	34
2	**Re-1**	5.5	99	63
3	**Re-2**	11	85	87
4	**Re-4**	7.5	96	55
5	**Re-5**	2.6	87	44

[a] Reaction conditions: pyridine *N*-oxide (100 μmol), catalyst (5 μmol, 5 mol%), DIPEA (570 μmol, 5.7 equiv.), CD_3CN (0.5 mL), 20 °C.

From a kinetic standpoint, the possible improvement of catalytic performances as pyridine was released was particularly noticeable in the case of 6,6′-substituted catalysts **Re-4** and **Re-5**. If their initial catalytic activities were low (TOF_0 = 7.5 and 2.6 h^{-1}), they showed steady catalytic activity past 2 hours of irradiation, while the conversion rates for the other catalysts were gently decreasing (Fig. 3b). This resulted in **Re-4** and **Re-5** reaching full conversion before **Re-1** and **Re-2**.

Several *para*-substituted pyridine *N*-oxides **1b–f** could be deoxygenated in 77–99% yield using photocatalyst **Re-3** (Fig. 4). The electronic parameters of the substituents affected the initial reaction rate: the yields after 30 minutes of irradiation evolved in line with the electron-withdrawing ability of the

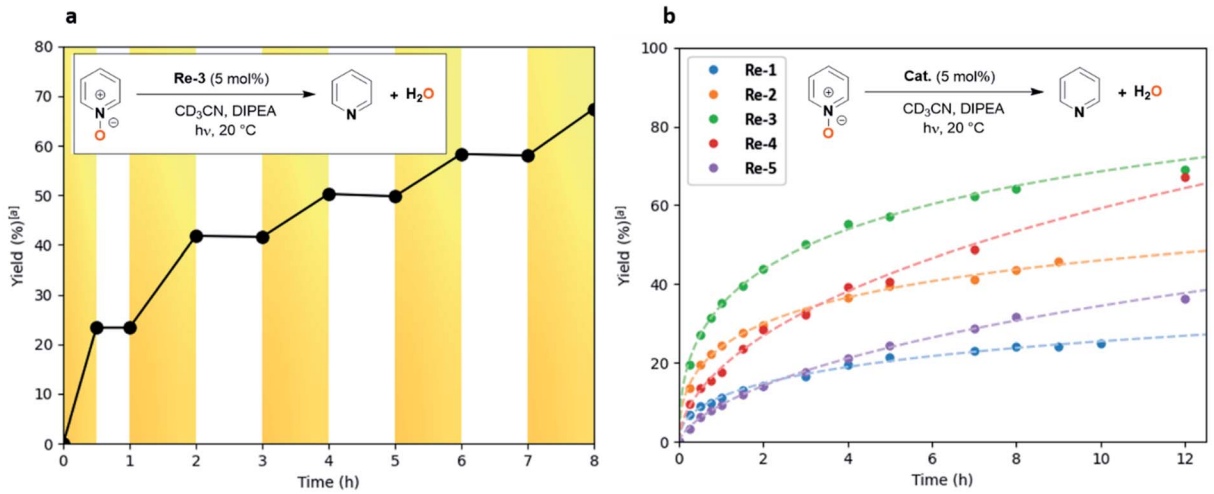

Fig. 3 Photoreduction of pyridine *N*-oxide. (a) Light and dark experiment with **Re-3**. Yellow: light on; white: light off. (b) Kinetic profiles of pyridine *N*-oxide photoreduction with different catalysts. Reaction conditions: pyridine *N*-oxide (100 μmol), catalyst (5 μmol, 5 mol%), DIPEA (570 μmol, 5.7 equiv.), CD_3CN (0.5 mL), 20 °C. [a]Determined by ^1H NMR analysis of the crude reaction mixture.

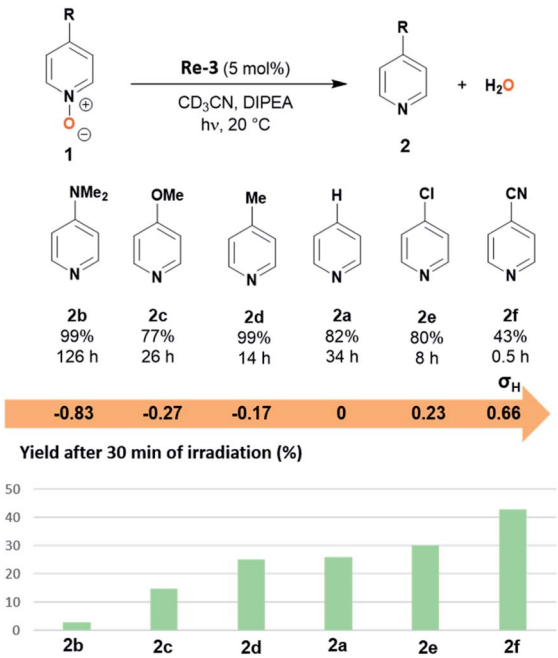

Fig. 4 Photocatalytic reduction of para-substituted pyridine *N*-oxides. (top) Scope of substrates (yield, time of irradiation until maximum yield). Corresponding Hammett constants of the substituents. Reaction conditions: pyridine *N*-oxide (100 μmol), **Re-3** (5 μmol, 5 mol%), DIPEA (570 μmol, 5.7 equiv.), CD_3CN (0.5 mL), 20 °C. Yields were determined by ^1H NMR analysis of the crude reaction mixture. (bottom) Yields of the photocatalytic deoxygenation of para-substituted pyridine *N*-oxides after 30 minutes of irradiation.

substituents as given by their Hammett sigma constants (Fig. 4b).[29] Indeed, compounds bearing electron-donating substituents were only poorly converted after 30 minutes: **1b–d** bearing dimethylamino, methoxy or methyl groups (σ_H = −0.83, −0.27 and −0.17 respectively) reached only 3 to 25% yield, while **1a**, **1e** and **1f**, bearing –H, chloro or cyano groups (σ_H = 0, 0.23 and 0.66 respectively) yielded after 30 min. 26, 30 and 43% of the corresponding pyridines, respectively. This was also reflected in the time to reach full conversion: pyridine *N*-oxides **1b-d** bearing electron-donating substituents (–NMe_2, –OMe, –Me) in the *para* position required longer reaction times (14–126 h) than **1e-f** with electron-withdrawing substituents (8 and 0.5 h respectively for the chloro and cyano derivatives). In particular the conversion of the nitrile derivative **1f** was extremely fast, maximal (43%) after only 30 minutes of irradiation. Further irradiation however led to over-reduction of **2f** to pyridine **2a** (for details see ESI Fig. S1†).

This is the first photocatalytic system able to perform such a deoxygenation reaction without additional energy sources. In contrast, strong reductants based on Hantzch esters or hydrazine were used by the groups of Konev and Wangelin[19c] and Lee.[19d]

In order to demonstrate the selectivity of this reaction and its synthetic utility, we explored the deoxygenation of a more complex substrate, a 2,6-substituted pyridine *N*-oxide. Pyridine *N*-oxide indeed features an enhanced reactivity compared to the reduced pyridine, enabling the functionalization of the 2,6-positions by C–H activation and, as an example, Hiyama *et al.* recently reported the synthesis of 2,6-substituted pyridine **3**, based on the oxidation of o-picoline to form the 2-methylpyridine *N*-oxide **4**.[30] A Ni-catalyzed coupling reaction leads to 2,6 substituted pyridine *N*-oxide **5**, whose deoxygenation presents multiple challenges that are chemoselectivity and steric hindrance. In their publication, the Hiyama group used PCl_3 as a reducing agent to perform such a deoxygenation. We were very pleased to observe that using our system, **Re-3** catalyzed the deoxygenation with 82% yield after 8 h of irradiation (Scheme 1). This demonstrates the validity of such an approach for mild deprotection strategies, which may be extended to other substrates.

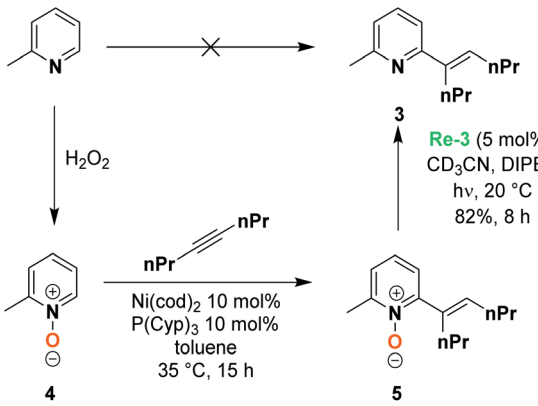

Scheme 1 2-Methylpyridine functionalization *via* the *N*-oxide strategy.

Conclusions

In summary, a new photochemical method has been developed to deoxygenate N–O bonds with radically different reduction potentials, over a 2.8 V window. [Re(4,4′-*t*Bu-bpy)(CO)$_3$Cl] (**Re-3**) is indeed capable of reducing both N_2O under ambient conditions, and pyridine *N*-oxides **1** and **4** in good to excellent yields. Those results open new perspectives concerning the photocatalytic deoxygenation of nitrogen oxide-containing compounds. Further mechanistic studies on catalyst **Re-3** are underway in our laboratory. We believe that these will provide new clues to understanding N–O bonds deoxygenation chemistry.

Data availability

Crystallographic data for [compound number] has been deposited at the CCDC under 2056048 and 2056049 and can be obtained from https://www.ccdc.cam.ac.uk/. The datasets supporting this article have been uploaded as part of the supplementary material.

Author contributions

MK and AO performed the investigations. PT performed the XRD analyses. EN, LAD and TC supervised the project. All authors contributed to the writing of the manuscript.

Conflicts of interest

There are no conflicts to declare.

Acknowledgements

We thank the CEA, CNRS, ERC (Consolidator Grant no. 818260), and Institut de France for funding. M. K. was supported by a Master fellowship from the LABEX Charmmmat followed by a PhD fellowship from ADEME. We thank Thierry Bernard (CEA) for his assistance in conception and realization of the photochemistry reactor.

Notes and references

1 A. Mosier, J. K. Syers and J. R. Freney, *Agriculture and the nitrogen cycle: Assessing the impacts of fertilizer use on food production and the environment*, Island Press, 2013.

2 (*a*) N. Lehnert, H. T. Dong, J. B. Harland, A. P. Hunt and C. J. White, *Nat. Rev. Chem.*, 2018, **2**, 278–289; (*b*) H. Tian, R. Xu, J. G. Canadell, R. L. Thompson, W. Winiwarter, P. Suntharalingam, E. A. Davidson, P. Ciais, R. B. Jackson, G. Janssens-Maenhout, M. J. Prather, P. Regnier, N. Pan, S. Pan, G. P. Peters, H. Shi, F. N. Tubiello, S. Zaehle, F. Zhou, A. Arneth, G. Battaglia, S. Berthet, L. Bopp, A. F. Bouwman, E. T. Buitenhuis, J. Chang, M. P. Chipperfield, S. R. S. Dangal, E. Dlugokencky, J. W. Elkins, B. D. Eyre, B. Fu, B. Hall, A. Ito, F. Joos, P. B. Krummel, A. Landolfi, G. G. Laruelle, R. Lauerwald, W. Li, S. Lienert, T. Maavara, M. MacLeod, D. B. Millet, S. Olin, P. K. Patra, R. G. Prinn, P. A. Raymond, D. J. Ruiz, G. R. van der Werf, N. Vuichard, J. Wang, R. F. Weiss, K. C. Wells, C. Wilson, J. Yang and Y. Yao, *Nature*, 2020, **586**, 248–256.

3 (*a*) J. Rockstrom, W. Steffen, K. Noone, A. Persson, F. S. Chapin 3rd, E. F. Lambin, T. M. Lenton, M. Scheffer, C. Folke, H. J. Schellnhuber, B. Nykvist, C. A. de Wit, T. Hughes, S. van der Leeuw, H. Rodhe, S. Sorlin, P. K. Snyder, R. Costanza, U. Svedin, M. Falkenmark, L. Karlberg, R. W. Corell, V. J. Fabry, J. Hansen, B. Walker, D. Liverman, K. Richardson, P. Crutzen and J. A. Foley, *Nature*, 2009, **461**, 472–475; (*b*) W. de Vries, J. Kros, C. Kroeze and S. P. Seitzinger, *Curr. Opin. Environ. Sustain.*, 2013, **5**, 392–402; (*c*) W. Steffen, K. Richardson, J. Rockstrom, S. E. Cornell, I. Fetzer, E. M. Bennett, R. Biggs, S. R. Carpenter, W. de Vries, C. A. de Wit, C. Folke, D. Gerten, J. Heinke, G. M. Mace, L. M. Persson, V. Ramanathan, B. Reyers and S. Sorlin, *Science*, 2015, **347**, 1259855.

4 (*a*) Electrochemical dinitrogen activation: To find a sustainable way to produce ammonia, S. Chen, S. Perathoner, C. Ampelli and G. Centi, in *Horizons in sustainable industrial chemistry and catalysis*, ed. S. Albonetti, S. Perathoner and E. A. Quadrelli, Elsevier, 2019, vol. 178, pp. 31–46; (*b*) O. Elishav, B. Mosevitzky Lis, E. M. Miller, D. J. Arent, A. Valera-Medina, A. Grinberg Dana, G. E. Shter and G. S. Grader, *Chem. Rev.*, 2020, **120**, 5352–5436.

5 J. G. Chen, R. M. Crooks, L. C. Seefeldt, K. L. Bren, R. M. Bullock, M. Y. Darensbourg, P. L. Holland, B. Hoffman, M. J. Janik, A. K. Jones, M. G. Kanatzidis, P. King, K. M. Lancaster, S. V. Lymar, P. Pfromm, W. F. Schneider and R. R. Schrock, *Science*, 2018, **360**, eaar6611.

6 (*a*) Y. Yamazaki, H. Takeda and O. Ishitani, *J. Photochem. Photobiol., C*, 2015, **25**, 106–137; (*b*) Y. Kuramochi, O. Ishitani and H. Ishida, *Coord. Chem. Rev.*, 2018, **373**, 333–356; (*c*) C. Chauvier and T. Cantat, *ACS Catal.*, 2017, **7**, 2107–2115.

7 (*a*) C. Costentin, M. Robert and J. M. Saveant, *Chem. Soc. Rev.*, 2013, **42**, 2423–2436; (*b*) H. Takeda, C. Cometto, O. Ishitani and M. Robert, *ACS Catal.*, 2016, **7**, 70–88.
8 D. R. Lide, *Crc handbook of chemistry and physics*, CRC press, 2004.
9 (*a*) V. N. Parmon, G. I. Panov, A. Uriarte and A. S. Noskov, *Catal. Today*, 2005, **100**, 115–131; (*b*) K. Severin, *Chem. Soc. Rev.*, 2015, **44**, 6375–6386.
10 R. Zeng, M. Feller, Y. Ben-David and D. Milstein, *J. Am. Chem. Soc.*, 2017, **139**, 5720–5723.
11 L. Anthore-Dalion, E. Nicolas and T. Cantat, *ACS Catal.*, 2019, **9**, 11563–11567.
12 T. Ming, R. de Richter, S. Shen and S. Caillol, *Environ. Sci. Pollut. Res.*, 2016, **23**, 6119–6138.
13 R. Deeba, F. Molton, S. Chardon-Noblat and C. Costentin, *ACS Catal.*, 2021, **11**, 6099–6103.
14 T. Kubota and H. Miyazaki, *Bull. Chem. Soc. Jpn.*, 1966, **39**, 2057–2062.
15 Y. L. Wang and L. M. Zhang, *Synthesis*, 2015, **47**, 289–305.
16 E. Howard and W. F. Olszewski, *J. Am. Chem. Soc.*, 1959, **81**, 1483–1484.
17 S. Chandrasekhar, C. R. Reddy, R. J. Rao and J. M. Rao, *Synlett*, 2002, 349–351.
18 H. P. Kokatla, P. F. Thomson, S. Bae, V. R. Doddi and M. K. Lakshman, *J. Org. Chem.*, 2011, **76**, 7842–7848.
19 (*a*) P. Xu and H. C. Xu, *Synlett*, 2019, **30**, 1219–1221; (*b*) Y. Fukazawa, A. E. Rubtsov and A. V. Malkov, *Eur. J. Org. Chem.*, 2020, 3317–3319; (*c*) M. O. Konev, L. Cardinale and A. Jacobi von Wangelin, *Org. Lett.*, 2020, **22**, 1316–1320; (*d*) K. D. Kim and J. H. Lee, *Org. Lett.*, 2018, **20**, 7712–7716.
20 J. Hawecker, J. M. Lehn and R. Ziessel, *J. Chem. Soc., Chem. Commun.*, 1983, 536–538.
21 (*a*) J. Hu, J. Wang, T. H. Nguyen and N. Zheng, *Beilstein J. Org. Chem.*, 2013, **9**, 1977–2001; (*b*) Y. Pellegrin and F. Odobel, *C. R. Chim.*, 2017, **20**, 283–295.
22 K. Kalyanasundaram, *J. Chem. Soc., Faraday Trans.*, 1986, **82**, 2401–2415.
23 V. W.-W. Yam, V. C.-Y. Lau and K.-K. Cheung, *Organometallics*, 2002, **14**, 2749–2753.
24 (*a*) J. M. Smieja and C. P. Kubiak, *Inorg. Chem.*, 2010, **49**, 9283–9289; (*b*) J. M. Smieja, E. E. Benson, B. Kumar, K. A. Grice, C. S. Seu, A. J. Miller, J. M. Mayer and C. P. Kubiak, *PNAS*, 2012, **109**, 15646–15650; (*c*) E. E. Benson, C. P. Kubiak, A. J. Sathrum and J. M. Smieja, *Chem. Soc. Rev.*, 2009, **38**, 89–99; (*d*) E. E. Benson and C. P. Kubiak, *Chem. Commun.*, 2012, **48**, 7374–7376.
25 As suggested by a referee, an alternative explanation would involve a change in the redox potentials of the catalysts leading to a change in the efficiency of the electron transfer.
26 As suggested by a referee, addition of chloride anions also improves the photocatalytic activity, in agreement with the findings of Lehn *et al.* in the photocatalytic reduction of CO_2. See ref. 27 and ESI† for more details.
27 J. Hawecker, J. M. Lehn and R. Ziessel, *Helv. Chim. Acta*, 1986, **69**, 1990–2012.
28 L. Buzzetti, G. E. M. Crisenza and P. Melchiorre, *Angew. Chem., Int. Ed.*, 2019, **58**, 3730–3747.
29 L. P. Hammett, *J. Am. Chem. Soc.*, 2002, **59**, 96–103.
30 K. S. Kanyiva, Y. Nakao and T. Hiyama, *Angew. Chem., Int. Ed. Engl.*, 2007, **46**, 8872–8874.